Experimental Evaluation of Theories for Trailing Edge and Incidence Fluctuation Noise

Martin R. Fink*
United Technologies Research Center, East Hartford, Conn.

Tests were conducted to evaluate conflicting theories for trailing edge noise and for incidence fluctuation noise. A flat-plate airfoil with flush-mounted surface pressure transducers was tested in an anechoic wind tunnel at velocities of 31.5-177 m/sec (108-580 fps) and nominal 4 and 6% grid-generated turbulence levels. In one series of runs, the airfoil was faired into the tunnel nozzle and extended beyond the nozzle lip for studies of trailing edge noise without a leading edge and with flow on only one side. Such noise was found to vary with velocity to the fifth power and turbulence level squared, as predicted by Ffowcs Williams and Hall and by Chase. Power spectral density at high frequencies decayed approximately inversely with frequency to the 10/3 power, as predicted by Chase. The data were poorly predicted by Hayden's correlation. Additional tests were conducted with the airfoil mounted on the tunnel centerline, with flow on both sides and turbulence convected past the leading edge. Surface pressure spectra caused by incidence fluctuations were reasonably predicted by the theories of Filotas and Mugridge at high frequencies, but were more closely predicted by that of Filotas at low frequencies. Far-field spectra decayed more rapidly than was predicted by their theory within a compact source analysis when the product of Strouhal number and Mach number was larger than about 0.5. Hayden's correction for acoustic noncompactness, which may also describe a phase cancellation effect on lift force, brought Filotas' theory into agreement with far-field spectra.

Nomenclature

a = speed of sound, m/sec
b = airfoil span, m
c = airfoil chord, m
$\bar{c}$ = effective radius of acoustic source, m
E = spectral density of mean square velocity fluctuation, m^2/sec
f = frequency, Hz
$\overline{F^2}$ = spectral density of mean square force, n^2/sec
k = reduced frequency, $\omega c/u$
L = ratio of integral scale length to half-chord, $2\Lambda/c$
$\overline{p^2}$ = mean square acoustic pressure, $(n/m^2)^2$
R = radial distance to far field, m
$\overline{S_E^2}$ = effective Sears function for lift response
St = Strouhal number, fc/U or $f\delta/U$
$\overline{u^2}$ = mean square streamwise velocity fluctuations, $(m/sec)^2$
U = streamwise mean velocity, m/sec
$\overline{v^2}$ = mean square transverse velocity fluctuation, $(m/sec)^2$
V = volume of turbulent eddy, m^3
W = width of trailing edge, m
δ = transverse correlation radius of turbulence, m
θ = angle from upstream direction to far-field measurement direction, deg
Λ = streamwise integral scale length of turbulence, m
ρ = density, kg/m^3
ω = angular frequency, $2\pi f$, rad/sec

Introduction

NOISE generated by solid bodies in the presence of engine airflow determines the inherent minimum noise of installed aircraft engines. For example, acoustically treated splitters within the engine inlet and exhaust ducts can attenuate turbomachinery noise but produce noise at their outer edges. Internal struts, necessary for structural support of the engine and splitters, are likely to be immersed in high-velocity turbulent engine airflows. In these and other instances, a solid surface of finite extent is in contact with airflow containing velocity and pressure fluctuations. The same basic aeroacoustic mechanisms should be present for all these examples; the magnitude of this noise should be predictable if airstream mean velocity, rms turbulence intensity, correlation lengths, and turbulence spectrum shape are known.

In some cases, different aeroacoustic analyses yield different predicted trends for the same kind of noise caused by convected turbulence. Each analysis contains some fundamental assumptions connecting turbulent aerodynamic flow to properties of the surface pressure fluctuations and connecting these to far-field acoustic radiation. If many of these quantities were measured, it would be possible to 1) accept some analyses as providing good agreement with data and 2) reject some analyses as clearly contradicted by data. Such tests and comparisons were conducted as part of NASA Lewis Research Center Contract NAS3-17863.

Comparison of Theories

Trailing Edge Noise

The earliest analytic solution for trailing edge noise was that of Powell,[1] who used dimensional analysis to examine several noise mechanisms associated with a turbulent boundary layer. Pressure fluctuations caused by turbulent eddies very near a sharp edge were assumed to have a transverse correlation length proportional to the ratio of speed of sound to characteristic frequency. Acoustic intensity was predicted to vary with flow velocity to the fifth power and turbulence intensity squared. Because turbulence intensity within a turbulent boundary layer was assumed to vary with Reynolds number to the -0.2 power, acoustic intensity was concluded to vary with flow velocity to the 4.6 power. Power spectral density was stated to vary inversely with frequency cubed at high frequencies.

Hayden[2,3] used essentially the same dimensional analysis but assumed that both the streamwise and transverse

Presented as Paper 75-206 at the AIAA 13th Aerospace Sciences Meeting, Pasadena, California, January 20-22, 1975; submitted January 27, 1975; revision received April 9, 1975. Sponsored by NASA Lewis Research Center, Contract NAS3-17863.

Index categories: Aircraft Noise, Aerodynamics (including Sonic Boom); Aircraft Noise, Powerplant.

*Senior Consulting Engineer, Aerodynamics. Associate Fellow AIAA.

correlation lengths were proportional to flow velocity. Thus he predicted a variation of acoustic energy with velocity to the sixth rather than fifth power. Acoustic intensity was predicted to be maximum in the upstream direction and was shown to have a distinctive directivity pattern given by $\cos^2(\theta/2)$ where θ is measured from upstream. Empirical curves were given [3] for spectra of trailing edge noise produced by three different flow regions. The resulting overall levels are not explicitly dependent on turbulence intensity.

Ffowcs Williams and Hall[4] calculated acoustic intensity of sound radiated by one turbulent eddy near the sharp trailing edge of a half-plane. Intensity was found to vary with velocity to the fifth power and turbulence level squared as with Powell's results[1] and to have the directivity predicted[2] by Hayden. Mean square acoustic pressure radiated by one eddy at a sharp edge was obtained as

$$p^2 = \pi^{-2}\rho^2 (U^5/a)(V/\delta^3)^2(\delta/R)^2(\overline{v^2}/U^2) \qquad (1)$$

where V is the volume and δ the transverse correlation radius of a turbulent eddy. To obtain edge noise for a trailing edge of span W, this result must be multiplied by the number of eddies at the trailing edge, which is proportional to $W/(2\delta)$.

Chase has obtained solutions[5] for sound power and spectrum shape as functions of detailed turbulence parameters. A fifth power velocity dependence was obtained. Power spectral density at large frequencies was predicted to vary inversely with frequency to the 10/3 power, in general agreement with the inverse cubed dependence predicted by Powell.[1]

Incidence Fluctuation Noise

Incidence fluctuations produced by upstream turbulence convected past an airfoil will cause fluctuations of lift force resulting in dipole noise. A prediction of overall power for such noise was obtained by Sharland[6] using a crude estimate for frequency-averaged equivalent lift curve slope. The sound spectrum was noted by Hayden[3] to be a product of three frequency-dependent effects: turbulence input spectrum, aerodynamic transfer function (lift response as a function of frequency), and acoustic transfer function. Numerous analytical solution are available for the lift force response of an airfoil to sinusoidal gusts, but only a few solutions have been extended to incident turbulence.

As a maximum limit on aerodynamic response, one can use the Sears function[7] for response to unswept gusts in incompressible flow. Then the lift force spectrum is given by

$$\overline{F^2}(\omega) = (\pi\rho U^2 Wc)^2 \overline{S^2}(\omega)\overline{v^2}(\omega)/U^2 \qquad (2)$$

and the Sears function can be approximated by

$$\overline{S^2}(\omega) = (1+2\pi k)^{-1} = (1+2\pi^2 \mathrm{St})^{-1} \qquad (3)$$

where k is the unsteady-aerodynamics reduced frequency $\omega c/(2U)$ and St is the Strouhal number fc/U. Turbulence is represented by a summation of gusts skewed at all angles relative to the airfoil. As shown analytically by Filotas,[8] lift force response per unit span is reduced for skewed gusts. Numerical solutions for lift force response to isotropic turbulence, per unit span, were given in Fig. 4 of his report.[9] Response was found to decrease with decreasing ratio L of turbulence integral length scale to airfoil half-chord and was approximately independent of reduced frequency at low reduced frequencies. Analytical approximations to those numerical solutions[9] were given as Eqs. (35) for small and large reduced frequencies; both equations give the same response at $k = 1/L$. High-frequency decay rate varies as k^{-1} for local loading and as k^{-2} for lift force response on a chordwise strip having small spanwise extent.

A different solution for lift force response in turbulence has been obtained by Mugridge.[10] Closed-form equations for the entire range of reduced frequencies were given as Eq. (3) for finite-span wings and Eq. (4) for two-dimensional airfoils. The two equations give aproximately the same response at large reduced frequencies. This lift force response decays inversely with frequency. At high frequencies it roughly agrees with that given by Filotas[9] for loading response. It does not have the larger decay rate expected for lift force as a result of phase cancellation. Calculated response at low frequencies is larger than is predicted by the low-frequency asymptotic solution of Filotas for two-dimensional airfoils.

The acoustic transfer function that relates acoustic mean square pressure fluctuation to lift force fluctuation was expressed by Hayden[3] for a noncompact acoustic source as his Eq. (13), which is

$$\overline{p^2}(\omega) = (4\pi Ra)^{-2}\{\omega^2[1+(\omega\bar{c}/a)^2]^{-1}\}\overline{F^2}(\omega) \qquad (4)$$

where $\bar{c}$ is an otherwise undefined effective radius of the acoustic source. The quantity in the inner square brackets is an approximate correction factor that approaches unity as the source becomes compact. In the limit of very small Strouhal number, both turbulence input spectrum and aerodynamic transfer function will be approximately independent of frequency, and the source will be compact. Power spectral density would then vary with frequency squared. For large Strouhal number, turbulence input spectrum and aerodynamic transfer function will both vary approximately inversely with frequency squared. At very low subsonic Mach numbers, calculated power spectral density at moderately large Strouhal numbers will vary inversely with frequency squared. For moderate subsonic Mach numbers and large Strouhal numbers the calculated acoustic transfer function will be independent of frequency, and power spectral density will vary inversely with frequency to the fourth power.

This type of rapid spectrum decay with increasing Strouhal number and moderate subsonic Mach numbers has been observed[11] in measurements taken directly above an airfoil. The decrease of high-frequency sound radiation below that calculated from measured surface loadings and the compact-source acoustic analysis was attributed[11] to a frequency-dependent correlation area. Another possible explanation, rather than acoustic noncompactness, might be an increased chordwise and spanwise phase cancellation of loading with increasing subsonic Mach number. Thus, the lift force spectrum at large products of Mach number and Strouhal number could be reduced below that for incompressible flow at constant Strouhal number.

Description of Experiments

Tests were conducted in the UARL Acoustic Research Tunnel.[12] This open-return wind tunnel has an open-jet test section within a chamber that is anechoic for broadband noise down to 200-Hz frequency. The 79×53 cm (31×21 in.) test section was 124 cm (49 in.) long. Models were supported by solid sidewalls; noise generated by the models could radiate through the upper and lower shear layer to microphones in the quiescent chamber. Grids could be installed upstream of the test section, in a region having 107 cm (42 in.) diam, to produce either of two turbulence levels in addition to the nominal 0.2% turbulence level. Turbulence intensities were spatially uniform in planes normal to the flow but decreased slowly with increasing downstream distance and increasing airspeed. Streamwise turbulence intensity at a distance 25 cm (10 in.) downstream of the nozzle was approximately given by

$$(\overline{u^2})^{1/2}/U = K(U/U_{\mathrm{ref}})^{-0.2} \qquad (5)$$

where the reference velocity U_{ref} is taken as 60 m/sec (200 fps) and the constant K was 0.06 and 0.04 for the two grids. Transverse (upwash) and streamwise intensities were approximately equal. Streamwise integral scale length obtained from autocorrelation of hot-wire measurements was 3.2 cm (1.25 in.) and spanwise integral scale length from cross-

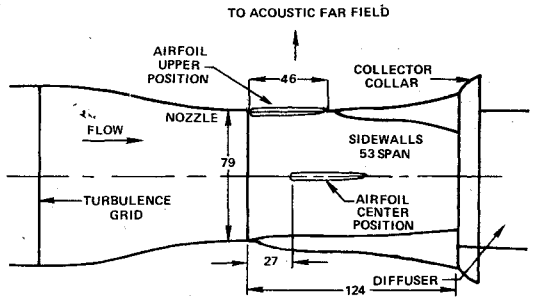

Fig. 1 Side view of acoustic tunnel test section. All dimensions in centimeters.

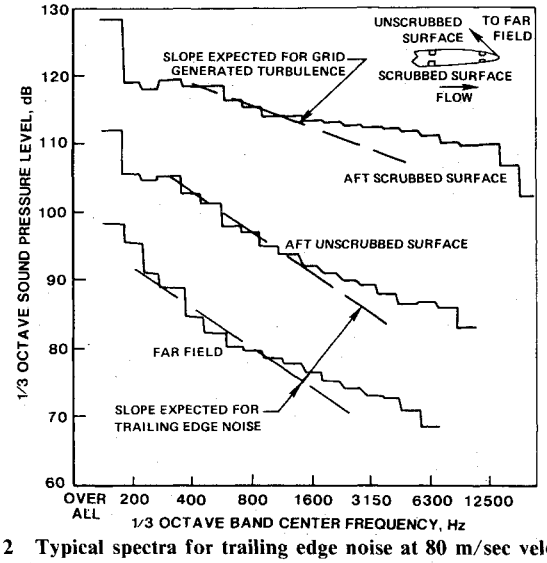

Fig. 2 Typical spectra for trailing edge noise at 80 m/sec velocity, large grid.

correlation of two probes at different positions was 1.9 cm (0.75 in.) for both grids over the range of velocities. Measured turbulence spectra E were in good agreement with predictions by Eq. (1-95) of Ref. 13

$$UE/(\overline{u^2}\Lambda) = 4[1 + (2\pi f\Lambda/U)^2]^{-1} \qquad (6)$$

using measured values of turbulence intensity, streamwise integral scale length, and mean velocity.

The airfoil model, which simulated a hard-wall splitter plate, had 46 cm (18 in.) chord and spanned the 53 cm (21 in.) width of the test section. It was 2.5 cm (1 in.) thick with a semicircular leading edge and a circular arc shape over the aft 6.4 cm (2.5 in.) and about 0.03 cm (0.01 in.) trailing edge thickness. Model thickness was chosen to allow easy installation of conventional Bruel & Kjaer 0.635 cm (¼ in.) condenser microphones, type 4136, on right-angle adaptors and preamplifiers. Microphones were flush-mounted without grids on both the upper and lower surfaces near the centerline at locations 5 cm (2 in.), 23 cm (9 in.), and 41 cm (16 in.) downstream of the leading edge. This model was tested at zero incidence at each of the two positions shown in Fig. 1. Trailing edge noise was examined with the airfoil leading edge faired into the test section nozzle exit lip, thus providing a trailing edge without a leading edge. For studying noise caused by incidence fluctuation, the airfoil was mounted at midheight of the test section, with its leading edge 27 cm (10.5 in.) downstream of the nozzle exit.

Wind-tunnel velocities for these tests were 31.5, 50, 80, 125, and 177 m/sec (103, 164, 262, 410, and 580 fps. The ratio of successive velocities thus differed by 1.6 except for the highest velocity, which had a ratio of 1.4. Maximum velocity was limited by loss of stagnation pressure at the grids; 200 m/sec (656 fps) velocity could be obtained otherwise. Microphones

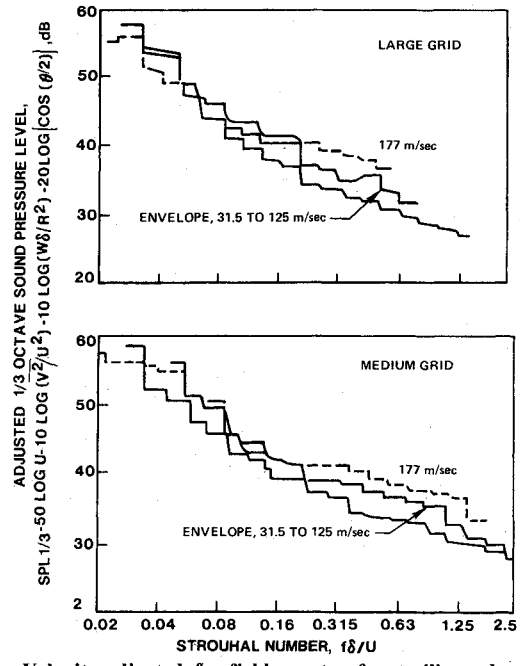

Fig. 3 Velocity-adjusted far-field spectra for trailing edge noise; velocity to the fifth power and turbulence level squared, direction 60° from upstream.

were located above the model at directions 60°, 90°, and 120° from upstream on an arc of 2.14m (7 ft) radius. Corrections to measured far-field sound caused by refraction of sound at the shear layer should be small[12] for lift dipole directivity and these angles. The microphone arc was centered at the trailing edge for studies of trailing edge noise and at mid-chord for incidence fluctuation noise. Far field sound pressure levels and surface pressure levels were measured in decibels re 2×10^{-5} n/m^2.

Comparison of Data and Theories

Trailing Edge Noise

Typical ⅓ octave spectra for aft positions on both surfaces, and in the far field 60° from upstream, are shown in Fig. 2 for 80 m/sec velocity and turbulence produced by the larger grid. The upper spectrum was measured at the aft microphone on the surface scrubbed by turbulent flow. These surface pressure fluctuations are a sum of the surface pressure spectra of grid-generated turbulence at low frequencies and boundary-layer turbulence, of much smaller scale and overall intensity, at high frequencies. At the same streamwise position on the unscrubbed surface (middle spectrum) and at other locations on that surface and in the far field, spectra were found to decay 6 db /octave as expected[1,5] for trailing edge noise. Background noise was not subtracted from the far-field spectra because the airfoil reduced the open jet length and thus reduced the background noise. Near-field trailing edge noise at a distance of about two streamwise integral scale lengths from the trailing edge (aft unscrubbed surface, Fig. 2) was about 15 db below the static pressure fluctuations of the convected turbulence (aft scrubbed surface). Cross-correlations between microphones on the scrubbed surface and those on the unscrubbed surface and in the far field had delay times consistent with convection of turbulence to the trailing edge at the flow speed plus acoustic propagation from the trailing edge.

According to the analyses of Ffowcs Williams and Hall[4] and of Chase,[5] far-field spectra should coalesce when ⅓ octave sound pressure level is decreased by 50 log U and 10 log $\overline{v^2}/U^2$ and frequency is plotted as Strouhal number. A plot of these spectra adjusted to a fifth-power velocity law for the microphone position 60° from upstream is given in Fig. 3. (In Figs. 3-5, the ordinate was calculated as if the velocity U,

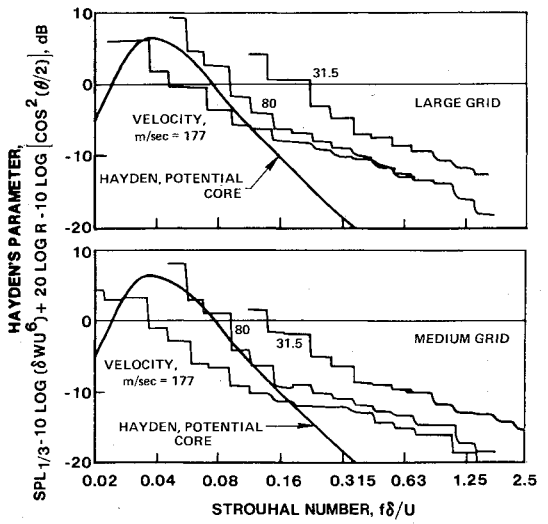

Fig. 4 Comparison of far-field trailing edge noise spectra with Hayden's prediction; velocity to the sixth power; direction 60° from upstream.

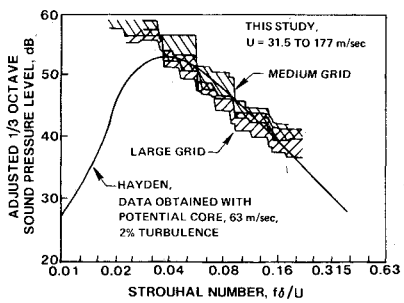

Fig. 5 Comparison of far-field trailing edge noise spectra adjusted for velocity to the fifth power and turbulence level squared.

m/sec, was a nondimensional number.) Spectra for a velocity ratio of 5.6 (a factor of 7.5 db) are brought into agreement by this scaling law. If data for the highest velocity at high frequencies (probably dominated by background noise) were omitted, agreement would be further improved. A comparison of these spectra with Hayden's[3] empirical curve for trailing edge noise in the potential core regime, which uses a sixth power velocity law, is given in Fig. 4. Data for different velocities and turbulence levels are spread apart. Trailing edge noise therefore varies with velocity to the fifth power and turbulence level squared, and is poorly predicted by Hayden's empirical method.

The data bands for these two turbulence levels and five velocities are overlaid in Fig. 5 to provide an empirical adjusted spectrum shape with a fifth-power velocity dependence. High measured levels at low Strouhal numbers may be caused by near-field effects. Data for high Strouhal numbers, shown in Fig. 3 and probably caused by tunnel background noise, are omitted from Fig. 5. Hayden's data[2] of Fig. IV.15 (a), which justified the empirical sixth-power curve[3] for the potential core flow regime, were then examined. Five of the seven spectra had been obtained at velocities between 61 and 64 m/sec (200 and 209 fps). This curve was assumed to give correct numerical results at 63 m/sec (206 fps) and was transferred to the adjustment parameters of Ffowcs Williams and Hall.[4] If 2% turbulence level is assumed for Hayden's data, this curve generally agrees with the other spectra, as shown in Fig. 5. The adjusted parameters for measured overall sound pressure level of these spectra was equal to 64. This overall level would be calculated from Eq. (1) if the average number of turbulent eddies at the trailing edge is assumed to be one-fourth the ratio of spanwise width to spanwise integral scale length.

To determine whether Hayden's far-field trailing edge noise data[2] were better matched by a fifth or sixth power law, data

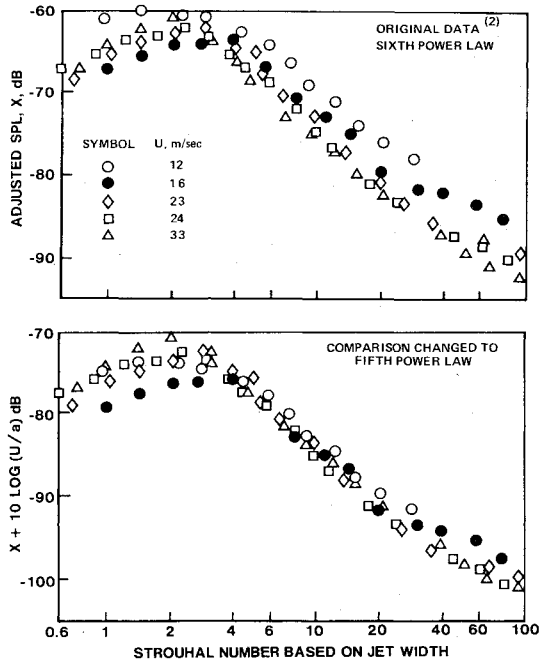

Fig. 6 Velocity power law comparison for Hayden's original far-field trailing edge noise data obtained in the radial decay flow region.

of Fig. IV.15 (c) for his radial decay regime were examined. Spectra for five velocities and constant plate length are reproduced in the upper part of Fig. 6 as taken from that figure with its assumed sixth power velocity dependence. Increased velocity reduced the measured values of adjusted SPL at constant Strouhal number. A fifth power comparison was obtained by adding 10 log (U/a) to each data point. The resulting plot, shown in the lower part of Fig. 6, approximately halves the scatter and intermixes spectra for different velocities. Therefore the data originally used by Hayden[2] for justifying a sixth power velocity dependence for trailing edge noise are in better agreement with the fifth power law predicted by Ffowcs Williams and Hall.[4]

Incidence Fluctuation Noise

Because surface pressure measurements on the upper and lower surfaces were not obtained at precisely the same spanwise position, signals could not be combined to yield local loading. The measured surface pressure spectra are a sum of pressure-coefficient response to incidence fluctuation and, at high frequencies, airfoil boundary layer turbulence. Previous tests[11] have shown that static pressure fluctuations and far-field noise due to incident turbulence are independent of mean angle of attack if the airfoil is not stalled, so this model was tested only at zero incidence. Several theories[9,10] predict different shapes of chordwise pressure response to turbulence. However, the ratio of local loading to chordwise-integrated lift coefficient as given by those two theories is roughly equal at midchord. One-third-octave surface pressure levels can be expressed in terms of frequency-dependent pressure response Cp_α and normalized turbulence spectrum E/U^2.

$$\mathrm{SPL}_s - 10\log(0.232f) = 20\log(\tfrac{1}{2}\rho U^2/p_{\mathrm{ref}}) + 10\log\overline{C^2_{P_\alpha}} + 10\log(E/U^2) \tag{7}$$

which can be rearranged as

$$\mathrm{SPL}_s - 20\log(\tfrac{1}{2}\rho U^2/p_{\mathrm{ref}}) - 10\log(\overline{v^2}/U^2) - 10\log(0.232\Lambda/c) = 10\log\overline{C^2_{P_\alpha}} + 10\log(fc/U) + 10\log(UE/\overline{v^2}\Lambda) \tag{8}$$

The left-hand side of Eq. (8) is a sum of a measured spectrum and terms that depend on velocity but not on frequency. The

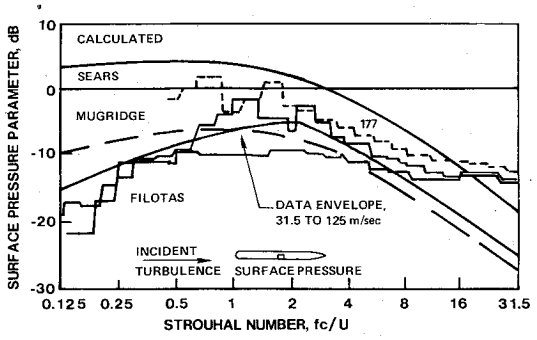

Fig. 7 Comparison of predicted and measured adjusted surface pressure spectra at mid-chord due to incidence fluctuation; large grid.

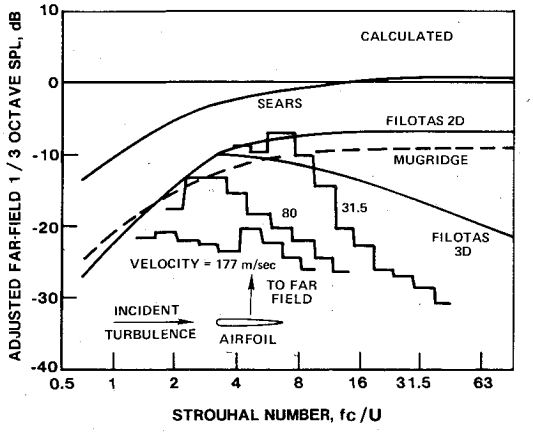

Fig. 8 Comparison of far-field incidence fluctuation noise spectra with compact source predictions; large grid; direction 90° from upstream.

right-hand side contains an analytical function of Strouhal number that can be calculated from different theories and two other functions of Strouhal number. In this comparison the left-hand side was determined from measured one-third-octave spectra by shifting amplitudes by the required amount and shifting frequencies of adjacent test points by 2 or 1½ third-octaves.

A comparison of adjusted surface pressure spectra at mid-chord for turbulence of the large grid is shown in Fig. 7. Spectra for the lower four velocities were in good agreement, while the spectrum for the highest velocity was consistently high. The portion of these spectra at Strouhal numbers above 5 is dominated by the airfoil turbulent boundary layer. As expected, pressure response calculated with Sears' theory[7] for unswept gusts overestimates the measured response to turbulence. The theory of Mugridge[10] for a low aspect ratio wing, neglecting the effect of the tunnel sidewalls, was arbitrarily used in an attempt to improve agreement with data. For this ratio of streamwise integral scale length to airfoil chord of 0.07, this and the theory of Filotas[9] agreed with data for Strouhal numbers larger than about one. The theory of Filotas, which uses separate equations for small and large Strouhal numbers, gave better agreement with surface pressure spectra at small Strouhal numbers.

The same type of data comparison used with surface pressure spectra was used for adjusting far-field ⅓ octave sound pressure levels. From Eqs. (2) and (4), the resulting equation for a compact source is

$$\mathrm{SPL}_{1/3} - 10\log(\overline{v^2}/U^2) - 10\log(0.232\Lambda/c)$$

$$-20\log(\pi\rho U^3 b\sin\theta)\,(2arp_{\mathrm{ref}})^{-1} = 10\log\overline{S_E^2}$$

$$+30\log(fc/U) + 10\log(UE/\overline{v^2}\Lambda) \qquad (9)$$

Measured spectra given by the left side of this equation are shown in Fig. 8 for three test velocities and the large grid.

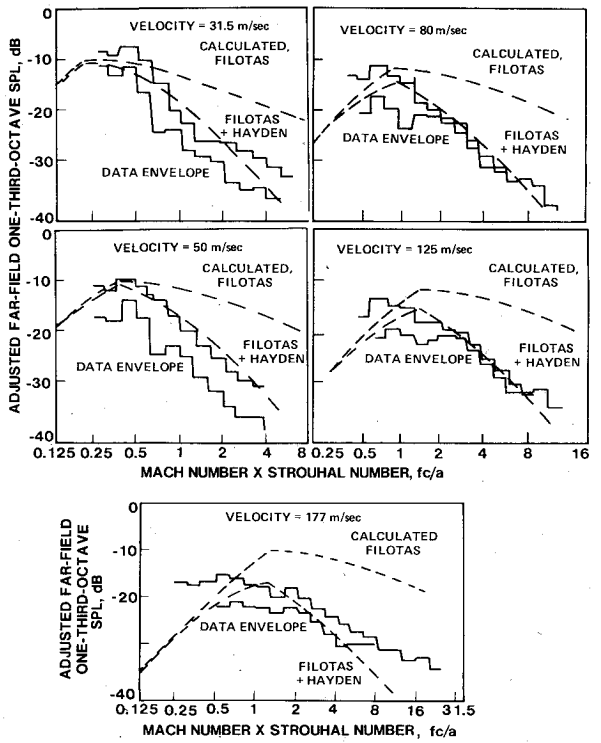

Fig. 9 Comparison of predicted and measured far-field incidence fluctuation noise spectra. Data envelope for measurement directions 60° and 90° from upstream at two turbulence levels.

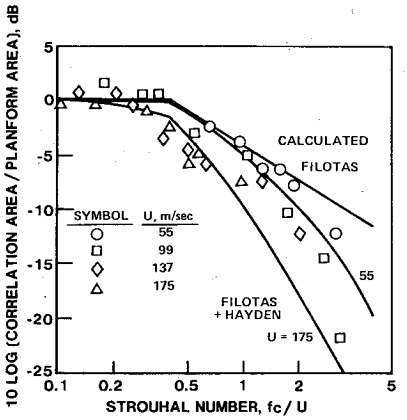

Fig. 10 Comparison of calculated predictions with Dean's results for far-field incidence fluctuation noise.

Tunnel background noise was subtracted from all incidence-fluctuation noise spectra. Clearly, this analytical approach, which assumes an acoustically compact source and no effect of compressibility on unsteady lift force response, does not produce agreement between far-field data taken at different velocities. Values for the right side of Eq. (9), as calculated from four incompressible flow analyses, are also shown. Sears' theory[7] for gust response overestimates the noise caused by turbulence-produced incidence fluctuation. The theories of Mugridge[10] for three-dimensional wings and Filotas[9] for two-dimensional loading neglecting spanwise variations give essentially the same prediction for the range of Strouhal numbers shown. Data tend to agree with these curves when the product of Mach number and Strouhal number is less than about 0.6, but are overestimated at larger values. The theory of Filotas[9] for lift force response on a narrow strip in incompressible flow improved qualitative agreement at the lowest velocity.

Hayden's[3] correction term was added to the comparison by subtracting the term $10\log[1+(\pi fc/a)^2]$ from the right side of Eq. (9). The effective radius of the source was arbitrarily

taken equal to half the chord. A comparison of resulting calculated and measured adjusted far-field ⅓ octave spectra for the five test velocities is shown in Fig. 9. The envelope of the four spectra measured by microphones 60° and 90° from upstream, and both turbulence levels, was adequately predicted at each velocity by combining Hayden's compressibility effect with the solution of Filotas.[9] Predicted and measured ⅓ octave spectra decay 9 db per octave at large Strouhal numbers.

Compressibility effects can be found in other measurements of noise from airfoils in turbulent flow. Tests reported by Dean[11] had included measurements of upstream turbulence spectra, loading spectra at the airfoil quarter-chord, and far-field acoustic pressure spectra. Turbulence integral scale length for those tests was about three times larger relative to chord than for the tests reported herein. As with these tests, local loading spectra were adequately predicted by the theories of Mugridge and Filotas. Fluctuating lift force was assumed in that study to be given by the product of local loading and a correlation area. Overhead far-field spectra and the compact-source acoustic dipole equation were then utilized to determine ratios of correlation area to planform area. The variation of this quantity with Strouhal number, taken from Fig. 14 of Dean's paper,[11] is shown in Fig. 10 for his four test velocities from 55 to 175 m/sec (180 to 575 fps). What had been described therein as a frequency-dependent correlation area can be calculated as a combination of incompressible-flow phase cancellation and Hayden's compressibility effect. Curves calculated for these two processes, again using an effective radius of half the chord, are shown in Fig. 10. Data for the lowest velocity were bracketed by the calculated curves for phase cancellation with and without the other effect. The decay with increasing Strouhal number was somewhat overestimated, but within about 4 db these data are predicted by the recommended calculation method.

Conclusions

Trailing edge noise varies with velocity to the fifth power and turbulence intensity squared, as predicted by Ffowcs Williams and Hall. Power spectral density decays roughly inversely with frequency cubed at high frequencies. Incidence fluctuation noise is predicted by using the theory of Filotas for lift force response combined with Hayden's factor for noise from noncompact acoustic sources.

References

[1] Powell, A.O., "On the Aerodynamic Noise of a Rigid Flat Plate Moving at Zero Incidence," *Journal of Acoustical Society of America,* Vol. 31, Dec. 1959, pp. 1649-1653.

[2] Hayden, R.E., "Sound Generation by Turbulent Wall Flow over a Trailing Edge," MS thesis, June 1969, Dept. of Mechanical Engineering, Purdue University, Lafayette, Ind.

[3] Hayden, R.E., "Noise from Interaction of Flow with Rigid Surfaces: A Review of Current Status of Prediction Techniques," NASA CR 2126, Oct. 1972.

[4] Ffowcs Williams, J. and Hall, L.H., "Aerodynamic Sound Generation by Turbulent Flow in the Vicinity of a Scattering Half Plane," *Journal of Fluid Mechanics,* Vol. 40, March 1970, pp. 657-670.

[5] Chase, D.M., "Sound Radiated by Turbulent Flow off a Rigid Half Plane as Obtained from a Wavevector Spectrum of Hydrodynamic Pressure," *Journal of Acoustical Society of America,* Vol. 52, Sept. 1972, pp. 1011-1023.

[6] Sharland, I.J., "Sources of Noise in Axial-Flow Fans," *Journal of Sound and Vibration,* Vol. 1, July 1964, pp. 302-322.

[7] Sears, W.R., "Some Aspects of Nonstationary Airfoil Theory and Its Practical Application," *Journal of Aeronautical Science,* Vol. 8, Jan. 1941, pp. 104-108.

[8] Filotas, L.T., "Theory of Airfoil Response in a Gusty Atmosphere. Part I-Aerodynamic Transfer Function," UTIAS Rept. 139, Oct. 1969, University of Toronto, Toronto, Ontario.

[9] Filotas, L.T., "Theory of Airfoil Response in a Gusty Atmosphere. Part II-Response to Discrete Gusts or Continuous Turbulence," UTIAS Rept. 141, Nov. 1969, University of Toronto, Toronto, Ont.

[10] Mugridge, B.D., "Sound Radiation from Aerofoils in Turbulent Flow," *Journal of Sound and Vibration,* Vol. 13, Nov. 1970, pp. 362-363.

[11] Dean, L.W., "Broadband Noise Generation by Airfoils in Turbulent Flow," AIAA Paper 71-587, June 1971, Palo Alto, Calif.

[12] Paterson, R.W., Vogt, P.G., and Foley, W.M., "Design and Development of the United Aircraft Research Laboratories Acoustic Research Tunnel," *Journal of Aircraft,* Vol. 10, July 1973, pp. 427-433.

[13] Hinze, J.O., *Turbulence,* McGraw-Hill, New York, 1959, p. 60.